Pergamon

Bioorganic & Medicinal Chemistry, Vol. 5, No. 2, pp 217–232, 1997

PII: S0968-0896(96)00229-5
0968-0896/97 $17.00+0.00

Modeling the Interaction Between FK506 and FKBP12: a Mechanism for Formation of the Calcineurin Inhibitory Complex

Michael T. G. Ivery* and Larry Weiler
Department of Chemistry, University of British Columbia, 2036 Main Mall Vancouver, British Columbia, Canada V6T 1Z1

Abstract—FK506 is a naturally occurring immunosuppressant whose mode of action involves formation of an initial complex with the cytosolic protein FKBP12. The composite surface of this complex then binds to and inhibits the protein phosphatase calcineurin (PP2B). To investigate why FK506 does not inhibit calcineurin directly we have conducted molecular modeling and conformational studies on published structures of FK506 both alone and in complex with FKBP12. From studies of the structure of FK506 in $CDCl_3$ and Z-Arg32-ascomycin in water (a water soluble analogue of FK506) we suggest that the FK506 molecule can be viewed as consisting of three separate regions. The pipecolate region which extends from C24 to C10 including the pipecolate ring shows strongly conserved conformation in both solvents. The loop region which extends from C25 to C16 shows general conservation of the loop structure and the pyranose region made up of the pyranose ring and C15–C17 which shows highly variable conformation depending on solvent. Comparison of the structure of Z-Arg32-ascomycin in water with structures of FK506 bound to FKBP12 indicate that the conformation of the pipecolate region is conserved during the binding process. The conformation of the loop region was generally conserved but a significant reduction ($\sim$1.7 Å) in the diameter of the loop in the bound structure was observed. The conformation of the pyranose ring and C15–C17 region was found to be significantly altered in the bound structure resulting in displacements of the C13 and C15 methoxyl groups of 2.8 and 3.5 Å, respectively. From computer models and molecular dynamics simulations of interactions between FK506 and FKBP12 we suggest that the conformational changes observed in bound FK506 are induced by the interaction between the 80's loop of FKBP12 and the pyranose ring of FKBP12. These interactions result in the formation of a complex with the both correct shape and surface polarity for interaction with calcineurin.

Introduction

In recent years significant insight has been developed into the biochemical pathways that connect antigenic activation of the T-cell receptor with lymphokine gene expression.[1] Particularly useful in the unravelling of these pathways has been the fungal metabolite FK506 (**1**),[2] which has recently received clinical approval for use in the prevention of organ rejection in transplant surgery and for the treatment of some autoimmune disorders.[3] FK506 acts at an intermediate stage of the signal transduction cascade by preventing the Ca^{2+} dependent activation of specific transcription factors (including NF-AT[4–6] and NF-IL2A[6]) involved in lymphokine gene expression.

FK506 is known[7–9] to induce its biological effects by interacting with two protein targets. The initial target for **1** has been identified as FKBP12,[10,11] which is one of a group of proteins known as immunophilins that are characterised by strong affinity for naturally occurring immunosuppressants and for their ability to catalyse the isomerisation of *cis*-proline residues in peptides and proteins (PPIase activity). This activity of FKBP12 is strongly inhibited by FK506.[10] However, it has been shown[12,13] using synthetic analogues of **1** that inhibition of the PPIase activity of FKBP12 is insufficient to induce immunosuppression. Thus, the role, if any, of this inhibition in the biological activity of these drugs is unclear. The second protein target for **1** has been identified[14] as the protein phosphatase PP2B calcineurin (CN),[15] which had not previously been implicated in signal transduction. The complex of FK506–FKBP12 was shown to bind tightly to CN[14] and to inhibit the phosphatase activity of this enzyme for synthetic and naturally occurring phosphopeptides. Neither **1** nor FKBP12 inhibit or bind to calcineurin alone.[14] The inhibition of CN is believed to prevent the translocation of the cytoplasmic component of NFAT (nuclear factor of activated T-cells) to the nucleus and thus prevent the formation of a competent transcription factor[4] for cytokine expression.

Insight into the nature of the interactions between **1** and its two protein targets have been gained from a range of structural determinations. Structural data on the FK506–FKBP12 complex[16,17] indicate that the region of **1** extending from C24 to C15 including the pipecolate and pyranose rings (see Scheme 1) makes intimate contact with FKBP12. The remainder of the molecule from C15–C23 which has been termed the 'effector loop',[18] protrudes outwards from the complex into solvent apparently ready for binding to CN. The pipecolate group is buried deeply within FKBP12 in a pocket lined with aromatic residues (Tyr26, Phe46, Phe48, Phe99, Trp59 and Tyr82) and hydrophobic

residues (Ile56 and Val55). The C24 hydroxyl and C1 carbonyl groups hydrogen bond to backbone carbonyl and amide groups of Glu54 and Ile56, respectively, in a fashion similar to antiparallel sheet interactions, which has led to the proposition that this region of FK506 can be viewed as a peptide mimetic.[16] Additional hydrogen bonds occur between C24 hydroxyl and Gln53 carbonyl (through a water molecule), Asp37 to the C10 hemiketal hydroxyl and Tyr82 hydroxyl to C8 amide carbonyl. Comparisons[18] of the X-ray structure of FK506 bound to FKBP12 with that of the solution structure of free enzyme[19,20] indicate that the core region of the protein described above does not undergo substantial conformational change on binding the FK506 ligand. However, two loop regions (Ser39–Pro45 and Tyr82–His87) appear to undergo both conformational and dynamical change. Both these loops occupy a definite conformation in the X-ray structure of FKBP12 bound to **1**,[16] however, in the solution structure of the free enzyme they are not well defined and may sample several conformations.[20] Initial comparisons[18] of the X-ray structure of free **1** with that of the FKBP12 bound molecule suggested that significant changes occur in the structure of **1** on binding to FKBP12. In particular, the C7—N8 amide bond of free FK506 was found to have *E*-stereochemistry while this bond is *Z*- in bound **1**. However, subsequent studies of solution structures of free **1** in $CDCl_3$[21] indicated that both *E*- and *Z*-conformers were present in solution. Furthermore, studies of a water soluble analogue of FK506, Arg32-ascomycin (**3**), indicated that the *Z*-conformer of **3** had a similar conformation to bound **1** and that FKBP12 selectively bound the *Z*-conformation of FK506.[22]

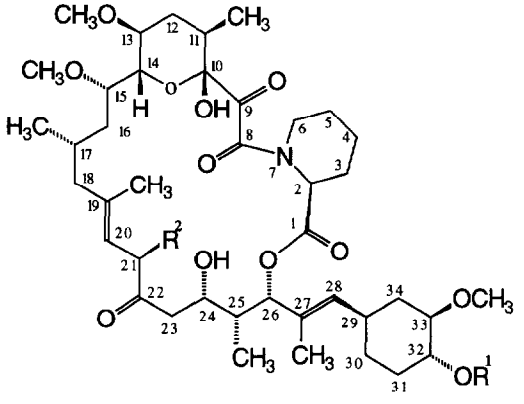

1 FK506 $R^1 = H$, $R^2 = -CH_2CH{=}CH_2$

2 Ascomycin $R^1 = H$, $R^2 = -CH_2CH_3$

3 Arg32-Ascomycin R^1 = Arginine, $R^2 = -CH_2CH_3$

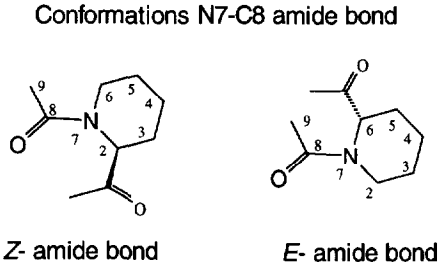

Scheme 1.

An X-ray crystal structure of the ternary complex of truncated CNA–CNB–FKBP12–FK506[23] and a low resolution structure of full length calcineurin bound to FKBP12 and FK506[24] have recently been reported. While the coordinates for these structures have not been made generally available, the binding of **1** into a hydrophobic cleft ~8 Å long between CNA and CNB on the surface of CN with the C21 allyl group of **1** deeply buried within CN was described. The conformation of **1** does not change on binding to calcineurin, but the molecule does rotate ~8° in the binding site of FKBP12 on complexation with CN. Other features of the complex included a large area of contact between CNA and FKBP and the observation that the binding site for the FK506–FKBP12 complex to CN is more than 10 Å from the active site of CN.

Additional information on the interaction of the FK506–FKBP12 complex with CN has been gained from structure–activity studies that show that even minor changes to the effector loop of **1** can greatly reduce the ability of the FK506–FKBP complex to inhibit CN even when binding of the modified **1** to FKBP12 is unaffected.[25] Structural comparison[26] of different FKBP's in complex with **1** and structure–activity studies of the interaction of **1** with mutant FKBP12[27] have indicated residues that are important to binding between **1** and FKBP12. In addition protein mutagenesis experiments on FKBP12 have identified specific residues that appear to be critical for the interaction of the FK506–FKBP12 complex with CN but do not affect the affinity of the mutant FKBP12 for **1**.[28,29] Also naturally occurring mutants of FKBP12 have been discovered that show strong affinity for **1** but whose complexes with **1** do not inhibit calcineurin. These inactive complexes could be made active by replacing specific residues with corresponding ones from FKBP12.[29,30]

A consensus view[7] on the interpretation of these experiments is that the biological activity of **1** is a two-stage process requiring an initial bonding between **1** and FKBP12 to form a composite surface. In the second stage of the interaction this composite surface then binds to calcineurin. The complete lack of affinity for CN by either **1** or FKBP12 alone suggests that both **1** and FKBP12 undergo conformational changes on formation of the FK506–FKBP12 complex and it is this new composite shape that is recognised by calcineurin. What is unclear is the specific nature of the modifications to each of the components of the complex which occur on binding to each other that are required for forming a complex capable of binding to calcineurin and how each partner in the complex induces these changes in the other.

In this paper we will use a range of conformational analysis techniques and computer-aided molecular modeling to analyse available structural information for **1** and FKBP12, both alone and in complex with each other. The aim of these studies is to define in detail the changes that occur to the structures of these molecules on formation of the complex and to rationalise these structural changes in terms of a mechanism for the interaction of **1** with FKBP12. Molecular dynamics simulations will be used to examine the proposed mechanisms for the interactions of FKBP12 and **1**. The rationalization of structure–activity relationships for mutated proteins will be discussed from the context of our proposed mechanism.

Results and Discussion

In attempting to define the structural changes that occur in FK506 (**1**) and FKBP12 on binding to each other, our initial approach was to examine the available structural data for **1** and FKBP12 both alone and in complex with each other. The aim of these studies was to identify regions of both molecules that maintained constant conformation in both the bound and free states. Subsequently these constant regions could be used both as reference points when comparing different conformations of **1** and FKBP12, and for the construction of computer models of the interaction of different conformations of **1** and FKBP12.

Conformational analysis of FK506

The stucture of FK506 (**1**) is a 21-membered macrocyclic ring with fused pipecolate and pyranose rings and a cyclohexyl substituent linked to the large ring via a *trans* double bond. In our structural analysis we exclusively examined the conformation of the 27-membered macrocyclic ring made up of the inner 21-membered ring and the two fused rings. Conformations of **1** can be grouped into two separate classes with either *E*- or *Z*- stereochemistry (see Scheme 1) about the amide bond between N7 and the C8 carbonyl. Ascomycin (**2**) is a naturally occurring anologue of **1** in which the C21 allyl group is replaced by an ethyl substituent. Ascomycin binds to FKBP12 with similar affinity to that of **1**, but the complex between **2** and FKBP12 is approximately twofold less active in inhibiting calcineurin. Both **1** and **2** are very hydrophobic molecules with very low solubility in water which precludes the determination of their solution structures in water. However, recently a water soluble analogue of **2**, Arg32-ascomycin (**3**) has been synthesised and its solution structure in water determined.[22] In the following analysis of the conformation of **1** we used the structure of this water soluble analogue to represent the structure of **1** in water. While it has been generally found that **1**–**3**[21,22] exist as a mixture of both *E*- and *Z*-conformers in solution, only the *Z*-conformer of **1** and **2** bind to FKBP12 and so in our study of the conformation of **1** we examined only this conformation.

The structures of *Z*-**1** in $CDCl_3$ and *Z*-**3** in water (representing *Z*-**1** in water) are shown in Figures 1(a,b), respectively. Each of these structures represent the molecule when viewed perpendicular to the mean plane of the macrocyclic ring. Figure 1c shows an overlay of these two structures for all 27 atoms of the macrocyclic, pipecolate and pyranose rings. The structures were overlaid by minimising the root mean square (rms) of the pairwise positional difference between corresponding atoms in the structures being compared. This analysis gives an RMS value in angstroms for the presented superposition with smaller values suggesting closer agreement between structures. For the comparison represented in Figure 1c the RMS value obtained was 2.59 Å.

This value suggests little similarity between these two structures. This has previously been rationalised[22] by invoking a solvent effect which can be illustrated in the structures shown in Figures 1(a,b). Comparison of these structures shows that in $CDCl_3$ (Fig. 1a) the pipecolate and pyranose rings extend outwards away from the macrocyclic rings toward solvent, while in water (Fig. 1b) these rings have collapsed inward under the macrocyclic ring. These differences are explained on the grounds of solvent effects in which the hydrophobic rings extend into the hydrophobic solvent, while in water the molecule tries to minimise the solvent accessible hydrophobic surface area.

A limitation of this RMS overlay analysis, however, is that in trying to minimise the pairwise differences between all atoms in the molecules any similarities in local areas of the molecules are sometimes obscured. To futher examine these structures of **1** with the aim to identify regions of conformational similarity we compared the corresponding dihedral angles of the macrocyclic rings in the two structures. To represent this comparison visually we constructed a plot (Fig. 2a) where the macrocyclic ring was represented by a ring divided into 27 segments with one segment for each bond in the ring. The segments were coded depending on the magnitude of the absolute difference in dihedral angle for that bond in structures of *Z*-**1** in $CDCl_3$ and *Z*-**3** in water.

Figure 2a shows that the conformation of *Z*-**3** in water and *Z*-**1** in $CDCl_3$ have very similar dihedral angles in the region from bond 23 (C24) past the cyclohexyl, pipecolate and dicarbonyl groups to C14. In this region only bonds 26, 1 and 9 have absolute differences in dihedral angle of more than 30°. Bonds 1 and 9 partly determine the orientation of the pipecolate and pyranose rings relative to the plane of the macrocyclic ring. The large difference in these dihedral angles indicates, as discussed above, that these rings are oriented differently with respect to the macrocyclic ring in the different solvents.

This analysis suggested that the high RMS value for overlay of the whole ring may stem from a difficulty in trying to accomodate different orientations of the pyranose and pipecolate rings in the two structures

rather than global differences in conformation. To futher investigate this possibility we divided the macrocyclic ring of **1** into two regions. One region which we will call the 'pipecolate' region extends from C24 past pipecolate and dicarbonyl groups to C10. The second region which we will call the 'loop' region extends from C25 past C21 to C16. We then repeated the RMS overlay analysis for the two structures, but only superimposing atoms in each of these regions. The results of the overlays for the pipecolate and loop regions are shown in Figure 2(b,c), and clearly show much better agreement between the two structures with RMS values of 0.41 and 1.02 Å, respectively.

In summary, this analysis suggests that **1** is made up of two regions of local conformation (pipecolate and loop) that are connected by a hinge region (pyranose ring and C15–C17). The pipecolate region displays a strong conservation of local conformation over a range of solvent polarities. The loop region retains its general loop appearance over a range of solvent polarity but shows significant variability within this loop in different solvents. The relative orientation of the pipecolate and loop regions is determined by the pyranose and the C15–17 region whose conformation varies widely depending on solvent.

Conformational analysis of FK506 bound to FKBP12

The structure of FK506 (**1**) bound to FKBP12 has been determined both in the solid state by X-ray crystallo-

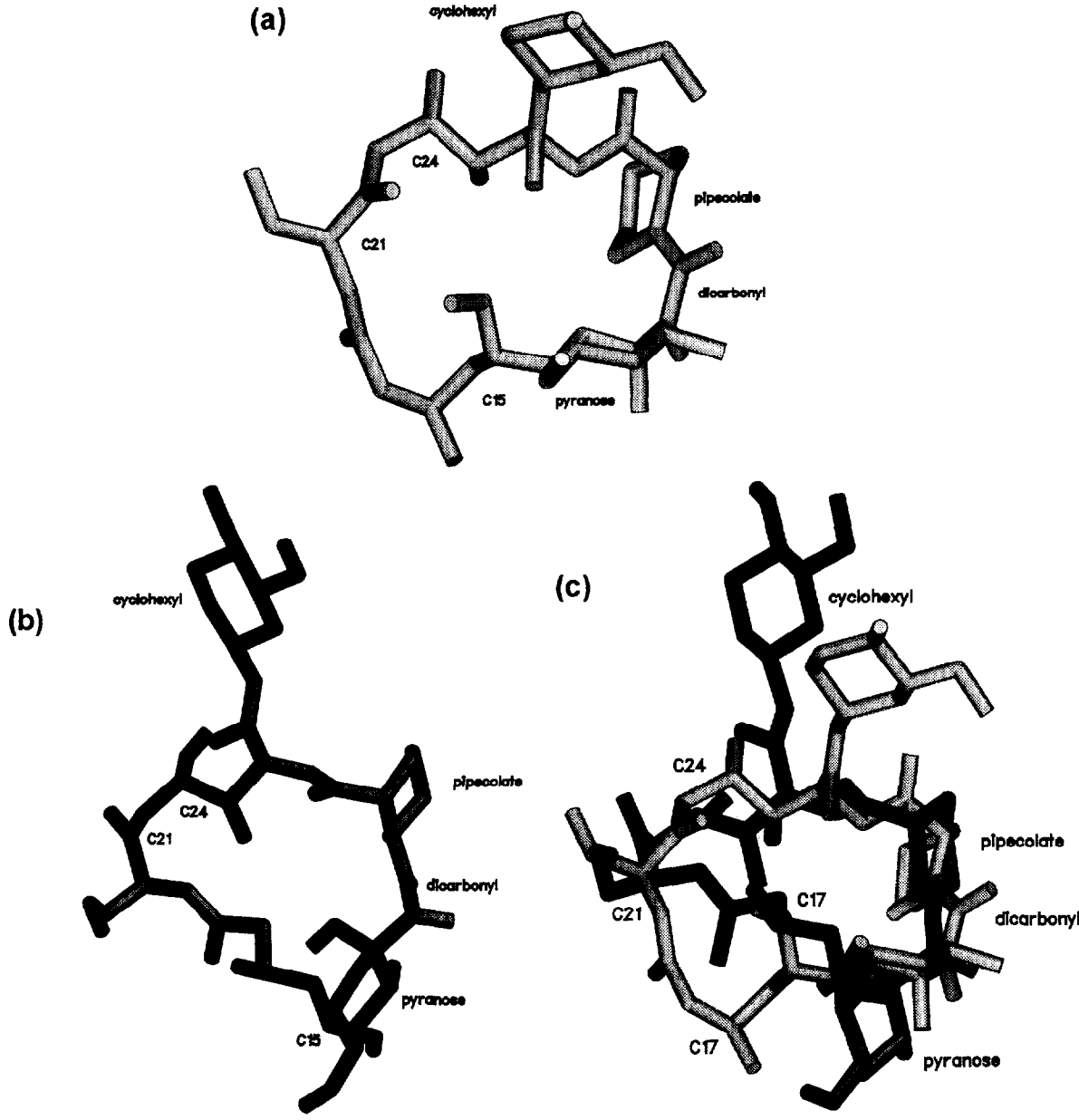

Figure 1. Comparisons of the solution structures of *Z*-FK506 (**1**) in $CDCl_3$ and water [represented by structure of *Z*-Arg32-ascomycin (**3**)]. Structures are viewed approximately perpendicular to the plane of macrocyclic ring. (a) *Z*-Arg32-ascomycin (**3**) in water (light grey) (Arg32 group is not shown); (b) *Z*-FK506 (**1**) in $CDCl_3$ (dark grey); (c) results of RMS overlay for structures displayed in (a) and (b) for all atoms in the macrocyclic ring of the two molecules including the fused pipecolate and pyranose rings.

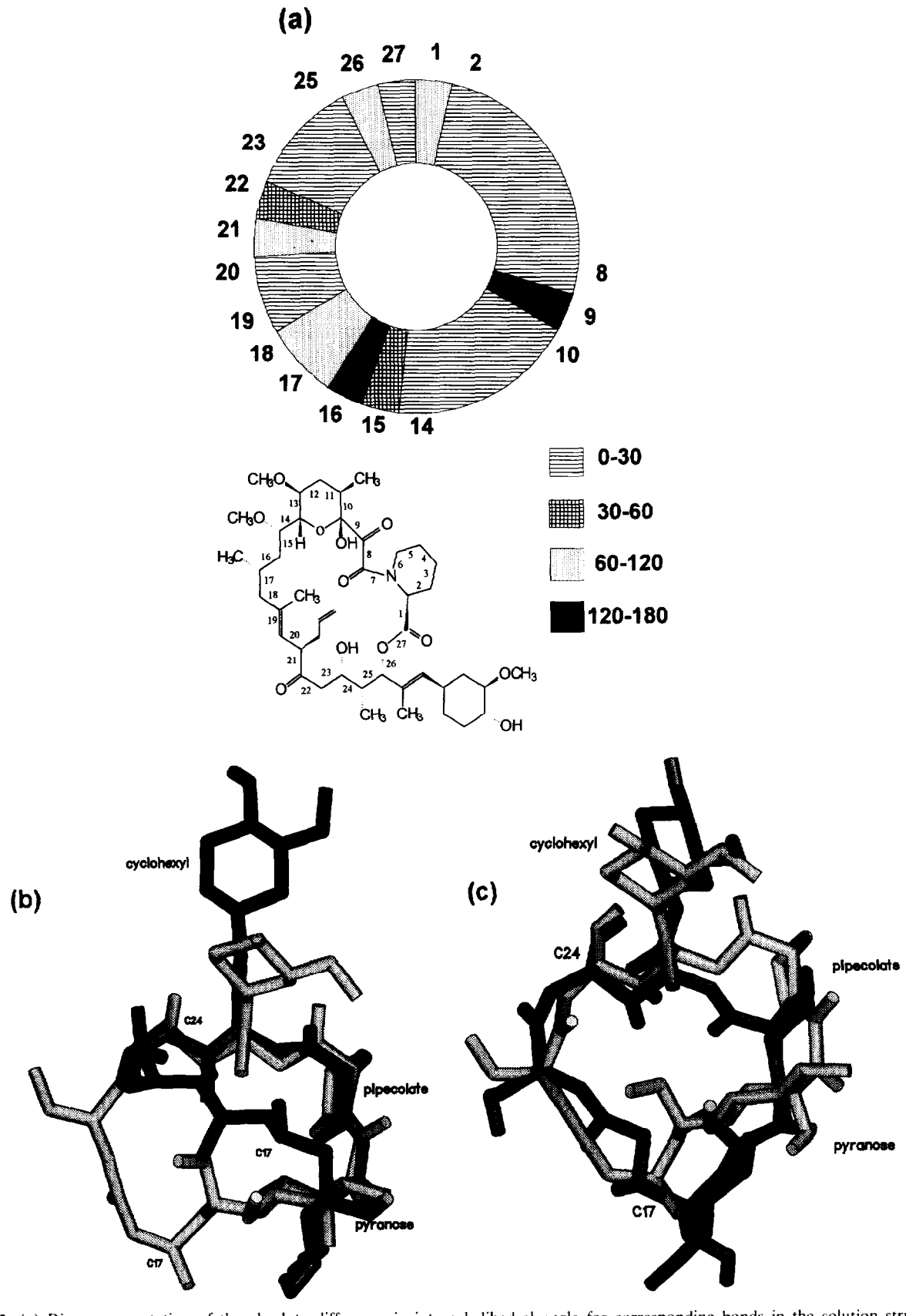

Figure 2. (a) Ring representation of the absolute difference in internal dihedral angle for corresponding bonds in the solution structures of *Z*-FK506 (**1**) in $CDCl_3$ and in water [represented by Z-Arg32-ascomycin (**3**)]. The ring represents the 27 bonds of the macrocyclic ring (bond numbering is on the structure). Each bond is coded for the magnitude of the difference in angle in the ranges 0–30, 30–60, 60–120, 120–180 degrees (see figure key). (b) Results of RMS overlay of the pipecolate regions (C24 to C10 past pipecolate and dicarbonyl groups) of *Z*-FK506 (**1**) in $CDCl_3$ and *Z*-Arg32-ascomycin (**3**) in water. RMS value for overlay is 0.43 Å. (c) Results of RMS overlay of the loop regions (C25 to C16 past C21) of *Z*-FK506 (**1**) in $CDCl_3$ and *Z*-Arg32-ascomycin (**3**) in water. RMS value for overlay is 1.03 Å.

graphy[16,17] and in solution by NMR.[31] Overlay of these structures indicate that all are very similar (Table 1, entries 1–3) with RMS values ranging from 0.12 to 0.28 Å for the whole ring, ~0.1 Å for the loop, and 0.09–0.27 Å for the pipecolate region. Comparison of dihedral angles for the macrocyclic ring in each of the structures show strong similarities with no differences greater than 30° between the X-ray structures and the NMR structure having only one bond (26) different by more than 30° with either of the X-ray structures. These results suggest that **1** when bound to FKBP12 has a narrow range of available conformations.

Comparison of conformations of FK506 free in solution and bound to FKBP12

To examine the changes if any that occur in the conformation of FK506 on binding to FKBP12 we conducted an RMS overlay comparison of *Z*-Arg32-ascomycin (**3**) (to represent the conformation of Z-FK506 alone in water solution) and the three structures of **1** bound to FKBP12. The RMS values for these comparisons (Table 1, entries 4–6) of the entire macrocyclic ring were in the range of ~0.9 Å (Fig. 3a), ~0.6 Å for the loop region (Fig. 3c) and ~0.2 Å for the pipecolate region (Fig. 3c).

These results show that the conformation of the pipecolate region is conserved during the binding process suggesting that this is a key element of structure that is recognised by FKBP12. Figure 3c shows the overlay of the loop regions of **1** bound to FKBP12 and of *Z*-**3**. The two structures are broadly similar in this region but the loop has a significantly smaller radius in the bound structure compared to the unbound. The distance across the loop from C16–C25 is ~4.9 Å in the free structure and ~4 Å in the bound structure and the distance from the C24 oxygen to C17 methyl is ~9.5 Å in the structure *Z*-**3** and ~7.8 Å in the FKBP12 bound structure of **1**. As discussed in the Introduction the binding of FK506–FKBP12 complex to calcineurin has been reported to involve the loop region of **1** being inserted into a surface cleft in calcineurin which was reported to be ~8 Å long, thus, the suggested larger diameter of the loop in **1** when unbound to FKBP12 may prevent the binding to this cleft and may be partially responsible for the complete lack of affinity of free **1** for calcineurin.

To compare further the structures of *Z*-**3** with **1** bound to FKBP12, the ring representation of the differences in dihedral angle for corresponding angles in the two structures was constructed and is shown in Figure 4a. This shows differences of more than 30° in only four torsional angles (14, 15, 16, and 21). The differences in bonds 14, 15, and 16 indicate that significant differences exist between the two structures in the region of the pyranose ring and C15-methoxyl group.

Figure 4b shows a comparison of the pyranose ring region of *Z*-3 and FKBP bound **1**. The figure was constructed by overlaying the pipecolate regions of the two molecules and then removing these regions to leave the pyranose and loop regions. This figure clearly shows differences in the orientation of the pyranose ring and atoms C15–C17 between the two structures. The differences between the two structures can be divided into two parts centering on the pyranose and C15–C17 regions, respectively. For the pyranose ring the differences between the two structures can be described by using C10 as a reference point. The pyranose ring of the bound structure is rotated in an anticlockwise direction using C10 as the center compared to the ring in the free structure (represented by *Z*-**3**) resulting in changes of the position of the C13 methoxyl of ~2.8 and 2.2 Å for the C11 methyl between the structures.

The second difference between *Z*-**3** (representing free *Z*-**1**) and FKBP12 bound **1** is shown in Figures 4b and

Table 1. Comparison of the structures of FK506 bound to FKBP12 with each other and with *Z*-Arg32-ascomycin

Entry	Structures Compared	Media/Technique	RMS[d] All[a]	RMS[d] Loop[b]	RMS[d] Pipecolate[c]	References
1	bound FK506 vs bound FK506	crystal/X-ray crystal/X-ray	0.12	0.13	0.09	16 17
2	bound FK506 vs bound FK506	crystal/X-ray solution/NMR	0.27	0.12	0.27	16 31
3	bound FK506 vs bound FK506	crystal/X-ray solution/NMR	0.28	0.10	0.27	17 31
4	*Z*-Arg32-ascomycin vs bound FK506	solution/NMR crystal/X-ray	0.86	0.63	0.21	21 16
5	*Z*-Ar32-ascomycin vs bound FK506	solution/NMR crystal/X-ray	0.91	0.59	0.23	21 17
6	*Z*-Arg32-ascomycin vs bound FK506	solution/NMR solution/NMR	0.89	0.54	0.21	21 31

[a]All is the RMS value for overlay of all ring atoms in the 21-membered macrocyclic ring and the fused pyranose and pipecolate rings.
[b]Loop is the RMS value for overlay of C25 to C16.
[c]Pipecolate is the RMS value for overlay of atoms C24 to C10 including dicarbonyl and pipecolate.
[d]RMS values are given in angstroms.

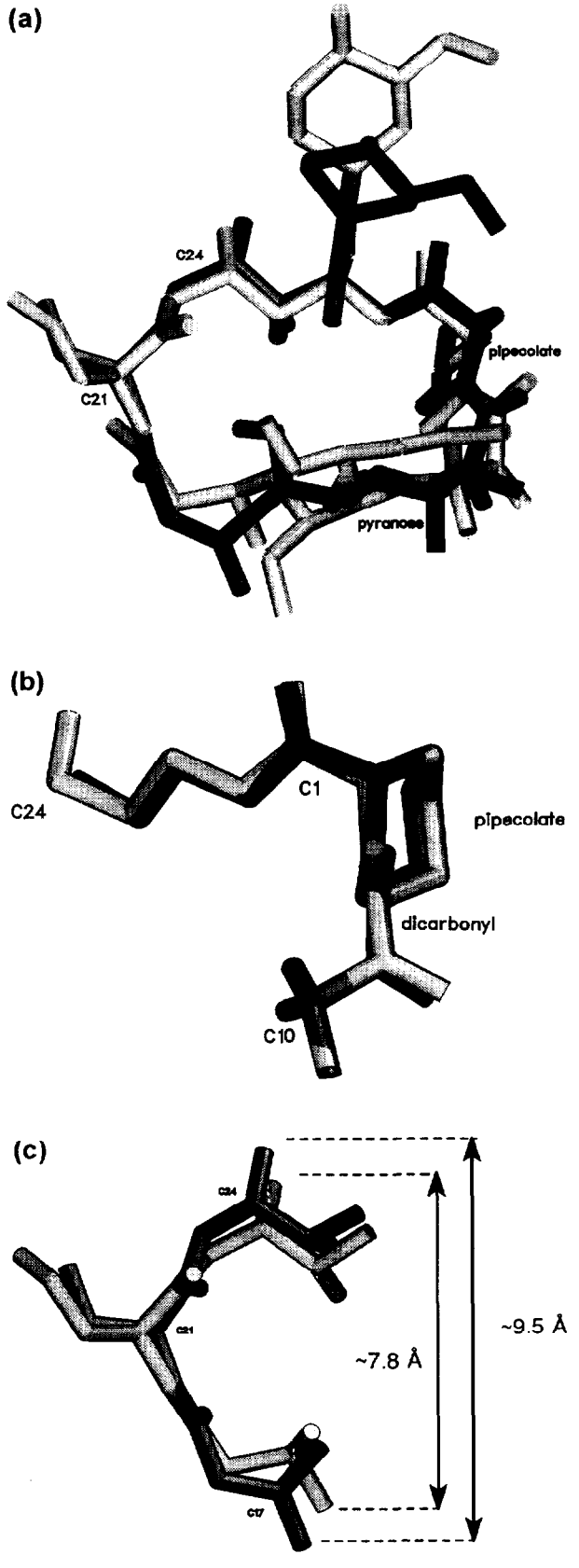

Figure 3. Results of RMS overlay of *Z*-Arg32-ascomycin (**3**) 22 (dark grey) with the structure of FK506 (**1**) (light grey) in the FK506–FKBP12 complex:[16] (a) for all of the 27-membered macrocyclic ring. RMS value for this overlay is 0.89 Å; (b) for pipecolate regions (C24 to C10 past pipecolate and dicarbonyl groups). RMS value for this overlay is 0.21 Å; (c) for loop regions (C25 to C16 past C21), RMS value for this overlay is 0.69 Å.

4c and involves the C13 and the C15 methoxyl groups. In the free structure the C15 methoxyl is oriented toward the center and above the plane of the macrocyclic ring in a g^+g^+ relationship with the C13 methoxyl group (Fig. 4c). This relationship of these two groups is maintained in all the published structures of unbound **1**.[2,21] In the bound structure, the C15 methoxyl has rotated out onto the periphery of the ring and is now in a g^+g^- orientation (Fig. 4c) to the C13 methoxyl. The rotation of the C15-methoxyl group is represented by the dihedral angle of C13–C14–C15–C16 which changes from 171° in the structure of *Z*-**3** to ~42–68° (X-ray and NMR structures) in the structure of bound **1**. This results in the two methoxyl groups being approximately coplanar in the bound structure of **1** (Fig. 4c). In the description of the structure of the complex between CN–FK506–FKBP12[23] it was noted that the C13 and C15 methoxyl groups of **1** form an unusual bifurcated H-bond with the Nε1 of Trp352 of calcineurin. This type of H bond interaction seems to be possible only for the orientation of the methoxyl groups observed in the bound structure. The movement of the C15 methoxyl results in a completely different orientation of the carbon chain at C16 pushing it inwards to form the tighter C16 to C25 loop in the bound structure as seen in Figure 4b. These effects result in displacement of the C16 methyl by ~1.7 Å and by ~3.5 Å for C15 methoxyl between bound and free structures.

The rotation of the C15 methoxyl group also has an effect on the nature of the surface that is presented to calcineurin by FKBP12. In its position in the bound structure of FK506–FKBP12 complex the C15 methoxyl group lies in van der Waals contact with the guanidine group of Arg42, the carboxylate group of Asp 37 and the hydroxyl group of Tyr26 this effectively shields these charged groups from direct interaction with calcineurin.

In summary, the above comparison of the structures of *Z*-**3** and FKBP12 bound **1** suggests that **1** has a region that remains conformationally unchanged (pipecolate region), a region that shows small changes (loop region), and a region that exhibits major changes (pyranose region) after binding to FKBP12. The conserved conformation of the pipecolate region during binding suggests that this is a key element of structure that is recognised by FKBP12. The structural changes observed in the pyranose and loop regions of **1** appear to be structurally related and result in the presentation of a conformation of **1** that is suitable for binding calcineurin.

Comparison of bound and free structures of FKBP12

Previously, it has been shown from both X-ray crystallography and molecular dynamics simulations[37] that portions of FKBP12 change conformation significantly on forming a complex with **1**. However it is also noted that portions of FKBP12 show strong conservation of conformation[18] during the binding process. These results are summarised in Figure 5. Figure 5a shows an

edited view of the binding site of FKBP12 bound to FK506 (1) taken from the crystal structure reported by Van Duyne et al.[16] This figure shows the hydrogen bonding of C24 hydroxyl with Glu54 carbonyl, the Ile56 amide with the C1 carbonyl, and the C10 hydroxyl with Asp37, along with the hydrophobic interactions between the pipecolate rings and Tyr26, Phe46, Phe48, Trp59, and Phe99. In this figure the side chains of Tyr26, Phe46, Phe48, Trp59, Ph99 and Tyr82 (not shown) and the backbone atoms of Glu54, Val55, and Ile56 of the free X-ray structure of FKBP12 have been overlayed to give an RMS value of ~0.4 Å. This overlay was also performed (not shown) using the same residues from the free solution structure to give an RMS of ~0.7 Å. In this figure we can see those elements of structure in both 1 and FKBP12 that remain unchanged during the binding process (i.e. pipecolate and hydrophobic core regions) interact with each other, suggesting that regions exist in both 1 and FKBP12 that are prearranged for binding.

Figure 5b shows an overlay of the protein aromatic cores for the X-ray structure of the FK506–FKBP12 complex and the solution structure of FKBP12 with the residues of the 40s and 80s loops ribboned and with side chains of Arg42, Asp37, His87, and Ile90 displayed. These loops have previously been identified as undergoing conformational and dynamical change on binding to 1 (see Introduction). This figure shows the movement of these loops on binding 1 which is

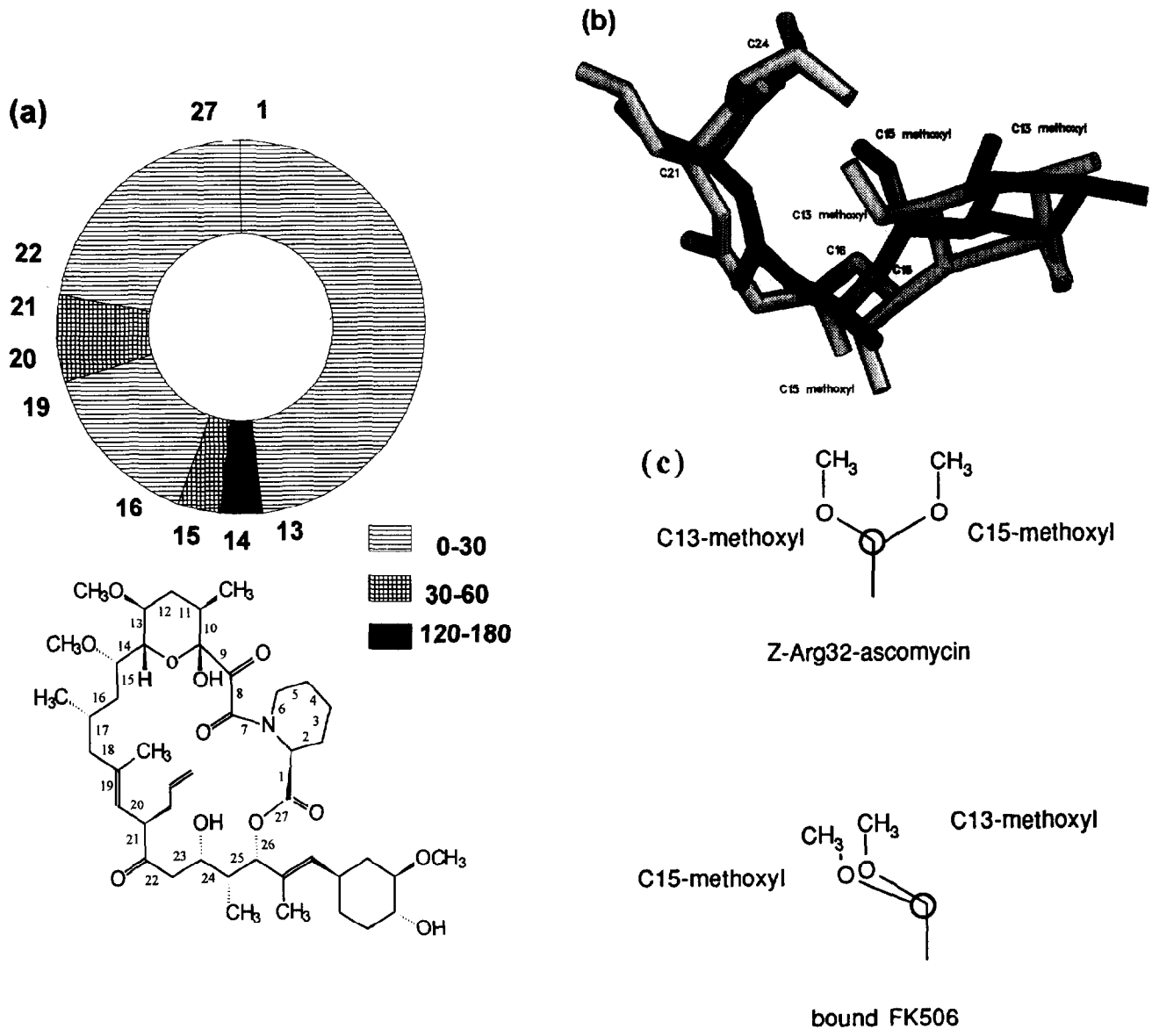

Figure 4. (a) Ring representation of the absolute difference in internal dihedral angle for corresponding bonds in the solution structures of Z-Arg32-ascomycin (3) in water and the structure of FK506 (1) in the FK506–FKBP12 complex.[16] The ring represents the 27 bonds of the macrocyclic ring (bond numbering is shown on the structure). (b) Comparison of conformation of pyranose ring regions in Z-Arg32-ascomycin (3) in water [used to represent free Z-FK506 (1) in water] and the structure of FK506 (1) in FK506–FKBP12 complex.[16] (c) Projection of the relative orientations of the C13 and C15 methoxyl groups in Z-Arg32-ascomycin in water and in the structure of FK506 in the FK506–FKBP12 complex. Dimensions marked on figures are in angstroms.

particularly illustrated by the movement of His 87 and Arg 42. His87 in the free structure of FKBP12 is ~9 Å from the C13 methoxyl group while in the bound structure this distance is ~4.4 Å. Similarly, the Arg42 guanidine group moves from being >9 Å from the C15 methoxyl group to being in van der Waals contact at a distance of ~3.8 Å in the bound structure. These observations indicate that the flexible regions of FKBP12 (40's and 80's loops) come into contact with the flexible regions of **1** (pyranose and C15-methoxyl regions) on binding to **1**.

In summary, this analysis of the conformations of **1** and FKBP12 both alone and in complex with each other indicate that each have certain regions that maintain their conformation during the binding process and other regions that change during binding. The regions that have conserved conformation in **1** and protein interact with each other suggesting that these regions are preorganised for binding. The regions that show conformational variability also interact with each other, which suggests that it is the mutual interaction between the two molecules during the binding process that results in the observed conformational changes.

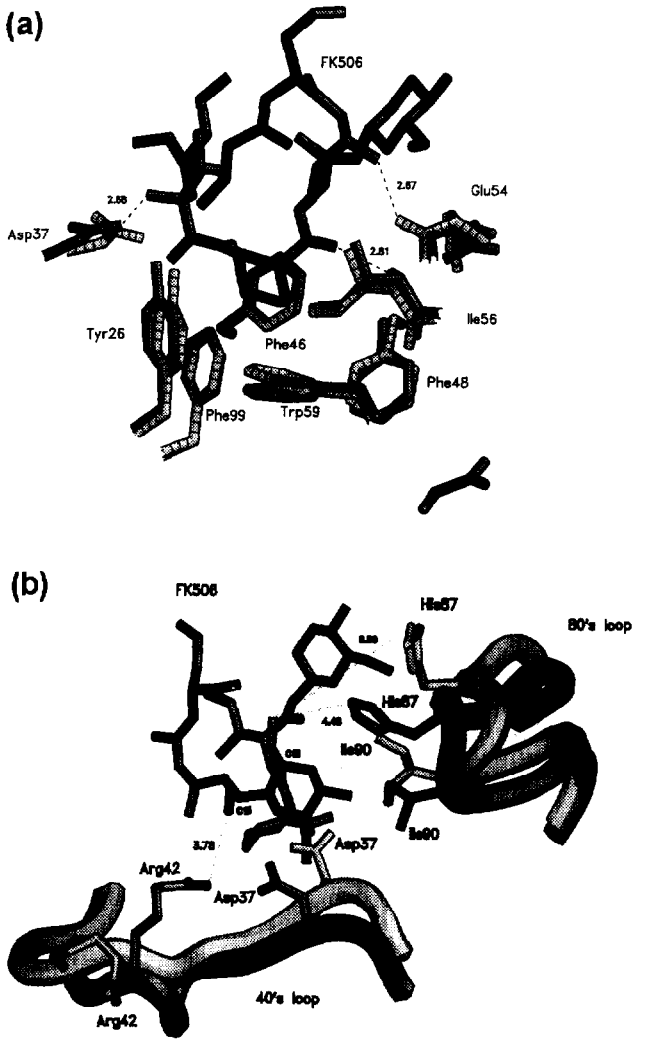

Figure 5. (a) Edited view of the FK506–FKBP12 complex[16] showing FK506 (black) positioned in the hydrophobic core of FKBP12 (dark grey). Overlaid on the displayed residues of bound FKBP12 (dark grey) are the coresponding residues in the X-ray structure of free FKBP12 (striped light grey). RMS value for this overlay is ~0.4 Å; (b) Edited view of the FK506–FKBP12 complex[16] showing FK506 (black) and FKBP12 (dark grey) with the side chains of His87, Arg42 and Asp37 displayed and the 40's and 80's loops ribboned. The solution structure of free FKBP12[19] (light grey) has been overlaid onto the FK506–FKBP12 complex using the same residues as in (b) for comparison. RMS value for this overlay is ~0.7 Å.

Modeling the interaction of FK506 with FKBP12

The above analysis uses the static experimental data on the structures of FK506 (**1**) and FKBP12 to define the structural changes that occur in each on formation of the complex between the two molecules. However, this analysis does not give any information on the dynamics of the interaction between the two molecules. That is, how does the interaction between the molecules result in the observed conformational changes? To investigate this question we took two approaches, one involving molecular models of experimentally inaccessible interactions between FK506 and FKBP12, and the second molecular dynamics simulations of FK506 and its interaction with FKBP12. Here we discuss some hypothetical molecular models we have constructed of different stages of the interaction of **1** and FKBP12.

The first model (Fig. 6a) is a representation of the first interaction of **1** and FKBP12 with both molecules in their unbound conformation. This model could be taken to represent the early stages of the interaction between **1** and FKBP12 showing the initial interaction between the aromatic residues of FKBP12 and the pipecolate ring of **1**. This initial, primarily hydrophobic, interaction is quite open to solvent with both the 40's and 80's loops of FKBP12 relatively remote from **1**. In particular His87 is ~5.5 Å from the C13 methoxyl group and Arg 42 is >6 Å from the C15 methoxyl group which is significantly different to the interaction of these groups in the bound structure (see Fig. 5a) where close van der Waals contact between these groups is found. This figure also shows that the two molecules are properly aligned for the formation of three hydrogen bonds between the pipecolate region C24 hydroxyl, the C1 carbonyl, and C8 carbonyl with Glu54, Ile56, and Tyr82, respectively. However, the disordered appearance of Asp37 suggests that the hydrogen bond between this group and the C10 hemiketal may form later in the binding process. Previously, structural and molecular dynamics studies[37] have indicated that the 40's and 80's loops of FKBP12 move as a unit on binding **1** to come into close contact with **1**. The expulsion of water from the predominantly hydrophobic binding site of FKBP12 has been proposed as the driving force for this movement. Some support for this hypothesis comes from a comparative thermodynamic and structural study of wild-type and mutant FKBP12 in complex with **1** which led to the conclusion that expulsion of two water molecules made a favorable contribution to the overall binding of **1** to FKBP12.[38]

To examine how the movement of the 40's and 80's loops of FKBP12 may induce the observed conformational changes in **1** when it binds to FKBP12. We constructed a model of the free **1** [represented by *Z*-Arg32-ascomycin (**3**)] in the binding site of FKBP12 with the enzyme in the bound conformation (see Experimental). This model is shown in Figure 6b and shows that the His87 residue of FKBP12 is now only ~1 Å from the C13-methoxyl group. In the actual structure of the FK506–FKBP12[16,17] complex (Fig. 5a) this same distance is ~4 Å. This suggests a possible mechanism for the conformational change in **1** on binding to FKBP12 where the C13 methoxyl group is displaced from its position in the free structure by the movement of the 80's loop. Figure 4b shows that the C13 methoxyl group in the bound structure occupies a very similar position to that of the C15-methoxyl group in the free structure. Thus the movement of the C13 methoxyl by the 80's loop could induce a subsequent displacement of the C15 methoxyl to its position in the bound structure. This mechanism is represented in diagramatic form in Figure 7. The rotation of C15 methoxyl group to the periphery of the ring results in a reorientation of the carbon chain of the macrocyclic ring from C16–C19 resulting in the formation of the tighter, more compact effector loop observed in the bound structure of **1** (Fig. 3c). Additionally, the rotation of the C15 methoxyl results in the methyl group sitting directly over the charged Arg42 and Asp37 groups effectively shielding the charged groups from direct interaction with calcineurin. Thus, in this mechanism we have a direct link between the binding of **1** to FKBP12 and the formation of a composite surface of FK506–FKBP12 with both the correct shape and surface polarity for interaction with calcineurin.

Some support for this mechanism can be taken from model studies on the complex of **1** bound to the double mutant H87V, R42K FKBP12. In this struture the His87 residue has been mutated to a valine residue.

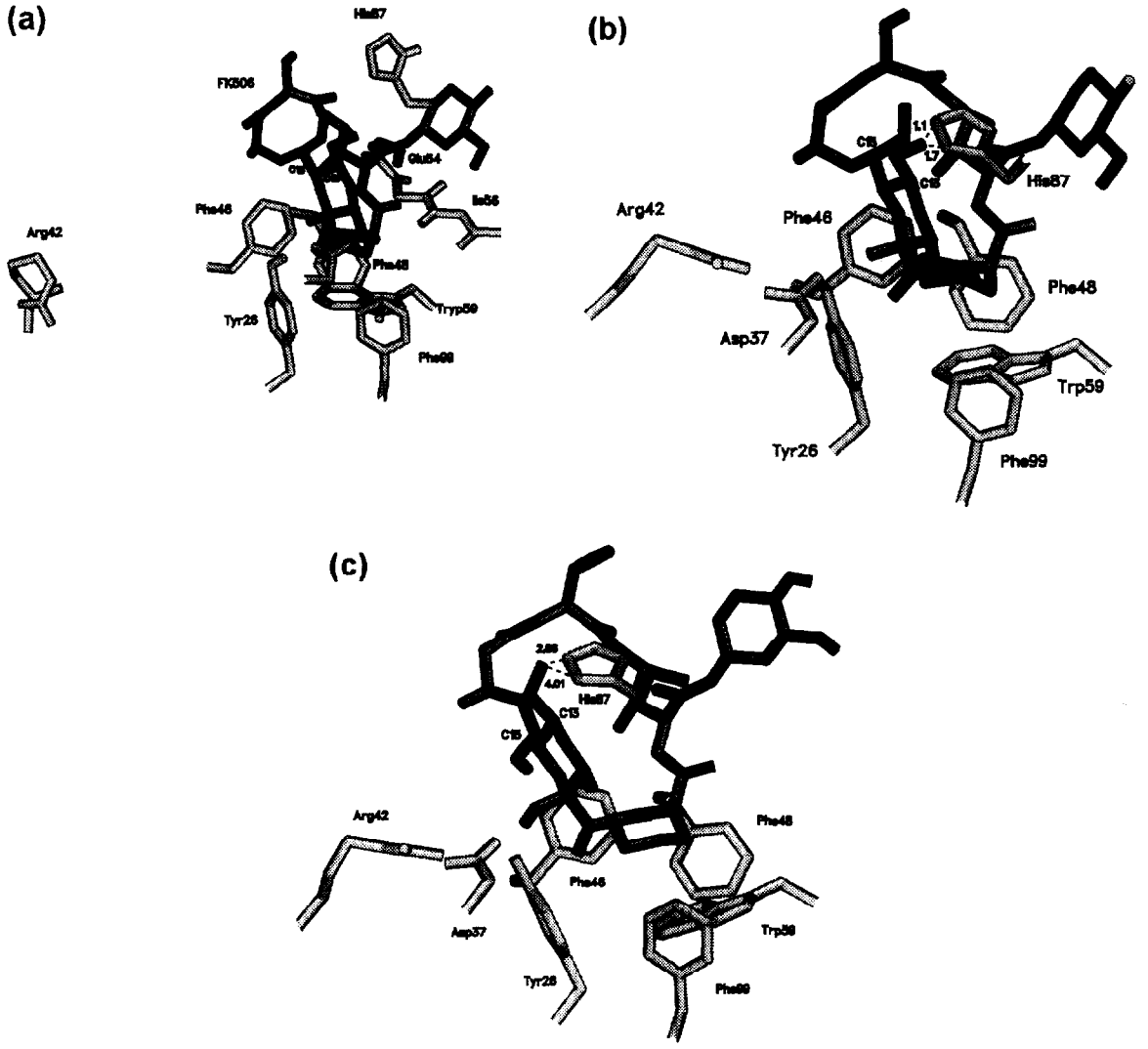

Figure 6. Models of interactions between FK506 and FKBP12. (a) *Z*-Arg32-ascomycin (**3**) in the FK506 binding site of the solution structure of FKBP12.[19] The relative positioning of the two molecules was achieved by overlaying the regions of the two molecules which have conserved conformation during the binding process. (b) *Z*-Arg32-ascomycin (**3**) in the FK506 binding site of the X-ray structure of FKBP12 in the FK506–FKBP12 complex.[17] (c) Solution structure of FK506 (bound to R42K, H87V double mutant FKBP12)[31] positioned in the binding site of the X-ray structure of FKBP12 in the FK506–FKBP12 complex.

We constructed a model of the structure of **1** bound to the double mutant enzyme[31] but located in the binding site of wild-type FKBP (see Experimental). This is shown in Figure 6c and shows the distance between the His87 residue and C13 methoxyl group as ~2.8 Å this is approximately 1.6 Å less than this distance in the structure of **1** bound to wild-type enzyme (Fig. 5b). This is as would be expected from the mechanism depicted in Figure 7 as the smaller valine residue in the mutant enzyme does not extend as far as the histidine residue in the wild-type enzyme and thus has not pushed the C13 methoxyl as far in the double-mutant complex.

However, in Figure 6c it is also noted that the C15 methoxyl is oriented below the plane of the macrocycle. The alteration of this group may result from the different conformation of the pyranose ring in this structure or from the replacement of Arg42 with a lysine residue in the double mutant. In the orientation displayed in Figure 6c the C15 methoxyl group does not sit on top of the Asp37–Tyr 26–Lys42 groups and so would not be expected to shield these charged groups from interaction with calcineurin. While the double mutant enzyme has similar affinity for FK506 to that of the wild-type enzyme the ability of this complex to inhibit calcineurin is ~680 times less than the complex of FK506 and wild-type FKBP12. This has previously been rationalised by postulating the presence of a direct interaction between Arg42 and calcineurin which is lost in the complex. However, our analysis suggests an alternative where the mutations result in a conformation of FK506 in the complex which does not shield the charge of the lysine residue (Lys42) and the loss of affinity is due to the introduction of an unfavorable interaction rather than the removal of a favorable one. Some support for this comes from additional protein mutagenesis studies which show that replacement of Lys44 with an alanine resulted in improved affinity for calcineurin by approximately eightfold.[27]

Molecular dynamics simulations on constrained FK506

The simplest interpretation of the mechanism depicted in Figure 7 involves two stages. In the first, the conformation of the pyranose ring region of FK506 (**1**) is altered on binding to FKBP12. This conformational change of the pyranose ring then induces a second conformational change in the C15 methoxyl group and further conformational changes in the effector loop.

In an attempt to both support the proposed mechanism and to possibly gain more insight into the mechanism we performed a series of molecular dynamics simulations on constrained **3**. The aim of these simulations was to examine whether the changes in conformation

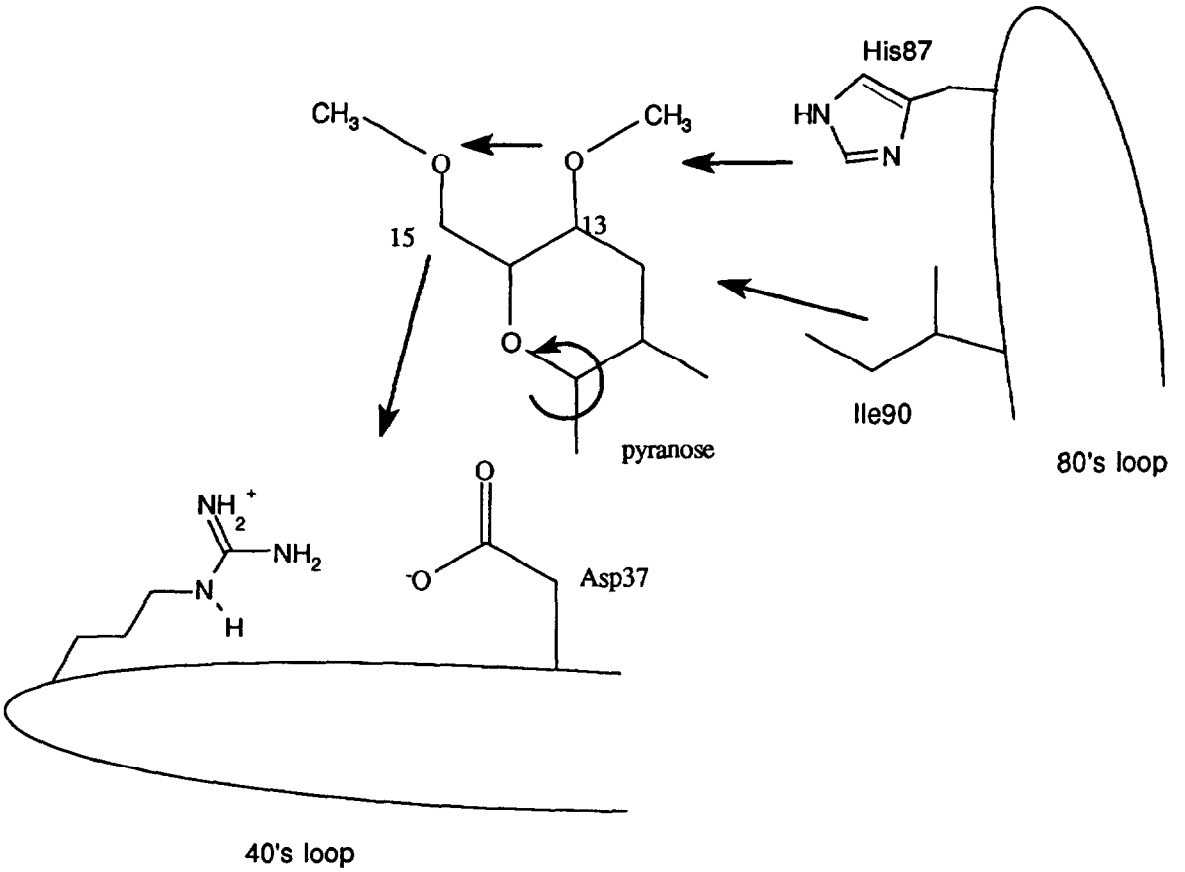

Figure 7. Schematic representation of the proposed mechanism for the interaction of FKBP12 and FK506 to form the final composite surface.

between bound **1** and free **3** in the pyranose and pipecolate regions were capable of inducing the observed differences in the C15 methoxyl and loop regions. To test this hypothesis we began with free **3** and using a series of atom constraints converted the conformation of the pipecolate and pyranose ring region to that observed in the bound structure of **1** during a molecular dynamics simulation (see Experimental). Figure 8 displays a stereo representation of the results of the simulation at 0.02, 0.1, and 5.0 ps. These figures show that as the C13 methoxyl is pulled into the bound position by the atom constraints it forces the C15 methoxyl group through the centre of the macrocyclic ring. This group continues its rotation after passing through the ring to finally finish in the same position as seen in the bound structure of **1**. In Figure 8d the results of a similar simulation where the pipecolate and pyranose ring regions of **3** were constrained to the conformation adopted by **1** when bound to the R42K, H87V double mutant enzyme (see Experimental) are displayed. In this case during the simulation the C15 methoxyl is again pushed through the ring but does not rotate as far as in the wild-type structure resulting in an orientation of the two methoxyl groups again very similar to that observed in the structure of **1** bound to the double mutant FKBP12.

Molecular dynamics simulations on constrained FK506–FKBP12 complexes

The above studies support the proposition that the conformation of the pyranose ring and pipecolate regions of FK506 (**1**) are controlling the conformation of the rest of the molecule. To examine whether it is the interaction between the loop regions of FKBP12 and **1** which results in the conformational change in **1** we performed a series of molecular dynamics simulations on constrained FK506–FKBP12 systems. The aim of these simulations was to begin with a model structure of free **1** [represented by *Z*-Arg32 ascomycin (**3**)] in the binding site of unbound FKBP12 and use atom constraints to both hold **1** in the correct orientation in the binding site and convert the free conformation of the enzyme into the bound structure.

Figure 9a shows a representation of the results of the above simulation after 100 ps. The resulting structure is overlaid in the pipecolate region with the bound structure of **1**. This figure clearly shows that the pyranose ring in the free structure has been rotated into the position of the bound structure by interaction with the moving 80's loop and in particular His87 and Ile90 which move in a pincer approach on the C13 methoxyl group. However, the strain between the C13 and C15 methoxyl groups in **3** is relieved not by a displacement of the C15 methoxyl but rather by an inversion of the conformation of the pyranose ring from a chair to boat-like orientation. This observation led to a second simulation where the conformation of the pyranose ring was constrained to the chair conformation. A stereo representation of the results of this calculation are shown in Figure 9b. Again the structure of bound **1** has been overlaid in the pipecolate region for comparison. In this figure the pyranose ring region of the bound structure and the simulation overlay almost exactly indicating that the interaction between the 80's loop of FKBP and the C13 methoxyl is sufficient to reorient the pyanose ring from the conformation seen in the free structure to that observed in the bound structure. In addition, the figure shows that the C13 methoxyl has moved into the space occupied by C15 methoxyl and displaced this group through the ring and this group now lies below the macrocyclic ring. However, the group was unable to rotate fully around due to obstruction by Tyr82 and Arg42. A possible explanation may require our simulation to take into account the known high mobility of the 40's loop to allow this group to settle into the correct position. Thus, we suggest that the controlling factor

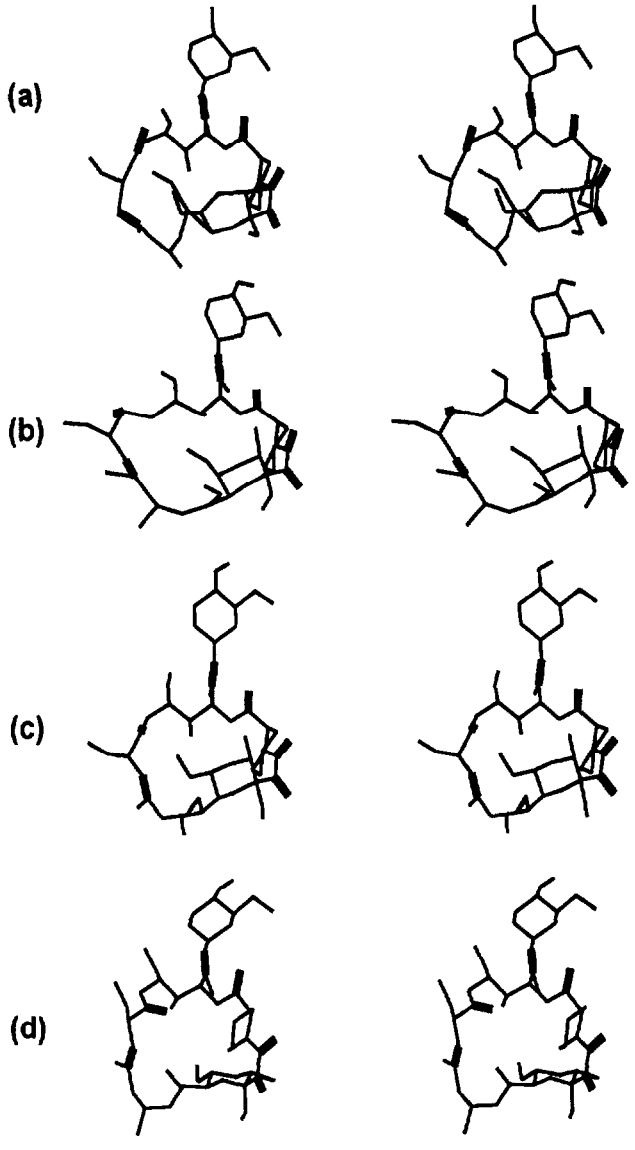

Figure 8. Molecular dynamics simulations on *Z*-Arg32-ascomycin (**3**) with atom constraints used to convert the conformation of the pipecolate region and pyranose ring into the bound conformation of FK506 during the course of the simulation. No constraints were applied to the loop or C15–C17 region. (a) Structure after 0.02 ps; (b) structure after 0.1 ps; (c) structure after 100 ps.

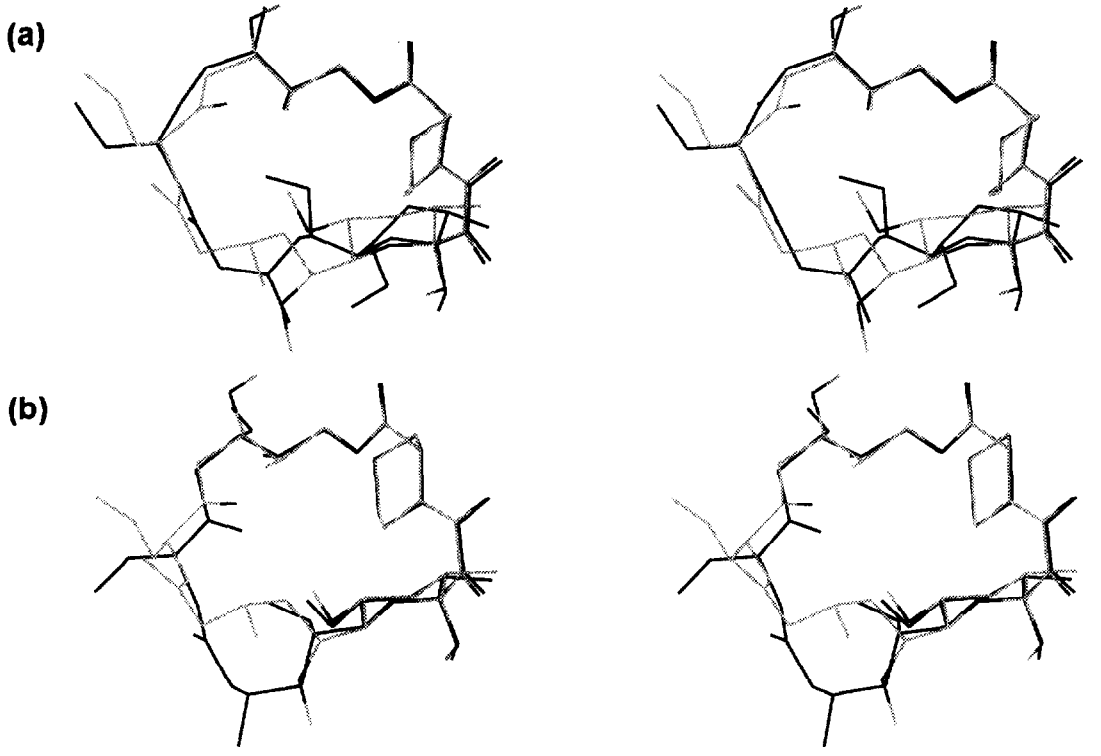

Figure 9. Comparison of result after 100 ps of molecular dynamics simulation on constrained *Z*-Arg32-ascomycin–FKBP12 complex (dark) with bound structure of FK506 (light). (a) Atom constraints used to transform the enzyme structure into that of the bound enzyme and the pipecolate region of the small molecule into the bound conformation. (b) Same as in (a) but additional constraints added to hold pyranose ring in starting chair conformation.

for the structure of the final complex is the interaction of the 80's loop and the C13 methoxyl group. Some support for this hypothesis is given by structural studies on complexes of FK506 with single mutant FKBP12's.[39] These studies showed that mutating His87 to a valine had a significant effect on the conformation of **1** when bound to the mutant enzyme but that the single mutation of Arg42 to lysine had a minimal effect on the structure of **1** bound to this mutant enzyme.

In discussing[31,39] these single mutant complexes some confusion has arisen because of the lack of correlation between the structural changes in the FK506–mutant FKBP12 complexes and the ability of the complexes to inhibit calcineurin. In particular, while the structure of **1** bound to the Arg42K mutant–FKBP12 shows little change in structure from the structure of **1** bound to the wild-type enzyme (RMS 0.14 Å),[39] this complex is ~170 times less active in inhibiting calcinurin than the wild-type enzyme. Conversely, the H87V mutant–FKBP12 complex shows a significantly higher difference in structure of the small molecule when compared to the wild-type complex (RMS 0.59 Å)[39] but only a approximately fourfold decrease in activity toward calcineurin. However, this may possibly be explained by our previous suggestion that the major effect of the R42K mutation is to introduce an unfavorable electrostatic interaction rather than a structural effect. The magnitude of such an unfavorable effect could be expected to much greater than that induced by modest structural changes. This is evidenced by the complete lack of affinity toward calcineurin displayed by the complex of 18-hydroxy **1** with FKBP12.[25]

Conclusions

We have presented a detailed conformational analysis of published structures of both FK506 (**1**), a water soluble analogue Arg32-ascomycin (**3**) and FKBP12. These structures were also compared with published structures of the FK506–FKBP12 complex and computer models of various stages of the interaction between **1** and FKBP12 were constructed. From these studies, we propose that while both **1** and FKBP12 have regions that appear to be prearranged structurally for binding to each other they also have regions that display significant conformational change on formation of the complex. Additionally, our computer models suggest that these variable regions in each molecule specifically interact with each other during the binding process and this interaction results in shaping the final structure of the complex.

We have proposed a mechanism for the structural formation of the FK506–FKBP12 complex that begins with an initial interaction between the structurally conserved pipecolate region of **1** with the hydrophobic core of FKBP12. Subsequently, driven by the entropic gain from the expulsion of water from the hydrophobic binding site, the 80's loop (~Ala95–Ala84) moves as unit hinging in to constrain the pyranose ring of FK506

into the bound conformation. This forces the C13 methoxyl group into the position occupied by C15 methoxyl forcing this group through the macrocyclic ring. The C15 methoxyl then rotates fully around to occupy its position in the bound structure. The 40's loop (Asp37–Pro45) then hinges in to seal off the binding site and complete the formation of the complex.

In the formation of the composite surface in the FK506–FKBP12 structure we have identified two structural modifications to **1** that may contribute to the gain in activity of **1** on formation of the complex. First, the loop region of FK506 clearly becomes more compact in the bound conformation of **1** compared to the free in solution conformation. Second, the orientation of the C13 and C15 methoxyl groups changes from g^+g^+ in the free structure to g^+g^- in the bound structure. Both those changes may play some role in the lack of affinity of free **1** for calcineurin. To examine this possibility we have designed compounds which mimic the bound conformation of **1**. These compounds are currently being prepared for biological evaluation.

Experimental

General

Molecular modeling was performed on a Silicon Graphics Indigo running under IRIX 5.2 operating system. Coordinates for the FK506–FKBP12[16,17] complex and for unbound FKBP12[17,19] were obtained from the Brookhaven Protein Data Bank. Coordinates for solution structures of FK506 (**1**) bound to wild-type FKBP12[31] and to the H87V, R42K double mutant FKBP12[31] were provided by Dr C. Lepre, Vertex Pharmaceuticals. Coordinates for solution structure of *Z*-**1** in $CDCl_3$[21] were provided by Dr R. Konat. Coordinates for solution structures of *Z*-Arg32-ascomycin (**3**) in water were provided by Dr A.M. Petros, Abbott Laboratories.[22] Comparison of structures by RMS overlay was performed using the SUPRA routine in the ANALYZ submode of MacroModel 4.5.[32] Other geometric calculations on structures including dihedral angles and atomic distances were measured using MacroModel 4.5. All molecular representations in Figures 1–6 were prepared using the molecular presentation program Setor[33] from coordinates ported to Setor from MacroModel. Figures 8 and 9 were prepared directly in MacroModel.

Energy minimizations and stochastic molecular dynamics simulations on **1** and FK506–FKBP12 systems were performed using the Batchmin program within MacroModel. The MacroModel implementation of the Amber force field was used in all calculations. This force field includes specific parameters for FK506 reported by Jorgenson et al.[34] For energy minimisation of model FK506–FKBP12 complexes the Polak–Ribiere conjugate gradient minimisation procedure was used. Solvent water was included in all calculations using the MacroModel implementation of the GB/SA model[35] which treats solvent as a fully equilibrated analytical continuum starting near the van der Waals surface of the solute. The SHAKE[36] algorithmn was invoked in all dynamics simulations with all bonds to hydrogen atoms constrained. All molecular dynamics simulations were conducted at an average temperature of 300 K.

Construction of models for the interaction of FK506 and FKBP12

Initially, a master file for creation of different models was created by overlaying the structures of *Z*-Arg32-ascomycin (**3**) (representing free FK506 in aq soln and free FKBP12[19]) onto the corresponding molecules in the structure of FK506–FKBP12[17] using the pipecolate region for reference to overlay the small molecules and the aromatic cores to overlay the proteins. Using this file a model of the interaction between free **1** [represented by Arg32-ascomycin (**3**)] and free FKBP12 (Fig. 6a) was created by deleting the structure of the FK506–FKBP12 complex. A model of the interaction between free **1** [represented by Arg32-ascomycin (**3**)] and **1** bound FKBP12 (Fig. 6b) was created by deleting the structure of **1** and unbound FKBP12 from the above master file. Figure 6c was created by overlaying the pipecolate regions of the structure of **1** bound to R42K, H87V double mutant FKBP12 with this region in the FK506-wild-type FKBP12 structure. The structure of **1** was then removed to leave the structure of **1** bound to R42K, H87V double mutant FKBP12 in the binding site of **1** bound wild-type FKBP12.

Simulations on constrained Arg32-ascomycin (3) molecules

Molecular dynamics simulations were performed on Arg32-ascomycin (**3**) [representing free FK506 (**1**)] using atom constraints to draw the pipecolate and pyranose ring regions of the molecule into the conformation of the bound structure of **1** during the simulation. To construct appropriate atom constraint files the structures of **3** and bound **1** were overlaid in the pipecolate region (C24 to C10). The structures of the two molecules were then saved separately to give two files where the coordinates for the pipecolate regions were very similar but differed in the loop and pyranose ring regions. A file of atom constraints was then constructed using the structure file for bound **1** and the MacroModel FXAT command (flat well 100 kJ constraint) selecting all the atoms in the pipecolate and pyranose ring regions. This constraint file was then used in a 200 ps simulation using the structure of **3** created above as starting geometry. Structures were sampled every 0.1 ps for the first 5.0 ps and then every 10 ps. The constraints were applied from the beginning of the simulation with constant strength and no other constraints were applied to the rest of the molecule. A 0.5 fs time step was used for the first 5.0 ps and then 2.0 fs time step for the remainder of the simulation. Debug flag 17 was invoked during the simulation to force the simulation to include interactions between constrained atoms. This procedure was repeated using

the structure of **1** bound to double mutant FKBP12 to create the constraint file. A 200 ps control simulation for unconstrained Arg32-ascomycin was also conducted.

Molecular dynamics simulations of FK506–FKBP12 systems

Molecular dynamics simulations of the interaction between FK506 (**1**) and FKBP12 were conducted as follows: a master overlay file was constructed in a similar fashion to that created in the construction of models for the interaction of FK506 and FKBP12, but using the X-ray structure for free FKBP12.[17] This file was then separated into two files, one containing the X-ray structure[17] of the FK506–FKBP12 complex and the other the model of Arg32-ascomycin (**3**) in the binding site of unbound FKBP12. Using the file for the FK506–FKBP12 structure an atom constraint file was created which defined **1** as the active substructure and also applied a 100 kJ flat well constraint to all atoms of FKBP12 within 10 Å of **1**. Also the atoms of **1** in the pipecolate region (C24 to C10) were constrained to their starting positions with a 100 kJ flat well constraint. The model structure of **3** in the binding site of free FKBP12 created above was then energy minimised for 500 steps with the protein structure constrained to the starting geometry. This minimised structure was then used as starting geometry for a 100 ps simulation where the atom constraint file created from the bound structure was applied to the model structure of **3** in the binding site of unbound FKBP12. For the first 5 ps, a time step of 0.2 fs was used and then 2.0 fs for the remainder of the simulation. This simulation had the effect of converting the conformation of FKBP12 from the unbound to the bound state. During this transformation **1** was held in the binding site of FKBP12 using atom constraints (100 kJ, flat well) to restrain the pipecolate region (C24 to C10) to the position of the bound pipecolate region. This simulation was then repeated with a futher constraint applied to the pyranose ring of **3** to hold the ring in the chair conformation using torsion angle constraints. Both simulations were sampled every 0.5 ps for the first 5.0 ps and then every 10 ps.

Acknowledgements

We would like to thank the Natural Sciences and Engineering Research Council, NSERC (Canada) for financial assistance and a Canadian International Fellowship (M.T.G.I), and Dr Lawrence McIntosh for provision of computer facilities.

References

1. Crabtree, G. R.; Clipstone, N. A. *Annu. Rev. Biochem.* **1994**, *63*, 1045.

2. Taga, T.; Tanak, H.; Goto, T.; Tada, S. *Acta Cryst.* **1987**, *C43*, 751.

3. Padova, F. E. *Persp. Drug Disc. Des.* **1994**, *2*, 49.

4. Rao, A. *Immunol. Today* **1994**, 15, 274.

5. Flanagan, W. M.; Cortes, B.; Bram, R. J.; Crabtree, G. R. *Nature (Lond.)* **1991**, *352*, 803.

6. Mattila, P. S.; Ullman, K. S.; Fiering, S.; McCutcheon, M.; Crabtree, G. R.; Herzenberg, L. A. *EMBO J.* **1990**, *9*, 4425.

7. Clardy, J. *Proc. Natl. Acad. Sci. U.S.A.* **1995**, *92*, 56.

8. Schreiber, S. L. *Science* **1991**, *251*, 283.

9. Thompson, A. W.; Starzl, T. E. *Immunolog. Rev.* **1993**, *136*, 71.

10. Harding, M. W.; Galat, A.; Uehling, D. E.; Schreiber, S. L. *Nature (Lond.)* **1989**, *341*, 758.

11. Siekierka, J. J.; Hung, S. H.; Poe, M.; Lin, C. S.; Sigal, N. H. *Nature (Lond.)* **1989**, *341*, 755.

12. Bierer, B. E.; Somers, P. K.; Wandless, T. J.; Burakoff, S. J.; Schreiber, S. L. *Science* **1990**, *250*, 556.

13. Somers, P. K.; Wandless, T. J.; Schreiber, S. L. *J. Am. Chem. Soc.* **1991**, *113*, 8045.

14. Liu, J.; Farmer, J. D.; Friedman, J.; Weissman, I.; Schreiber, S. L. *Cell* **1991**, *66*, 807.

15. Klee, C. B.; Krinks, M. H. *Biochemistry* **1978**, *17*, 120.

16. Van Duyne, G. D.; Standaert, R. F.; Karplu, P. A.; Schreiber, S. L.; Clardy, J. *Science* **1991**, *252*, 839.

17. Itoh, S.; Decenzo, M. T.; Livingston, D. J.; Pearlman, D. A.; Navia, M. A. *Bioorg. Med. Chem. Lett.* **1995**, *5*, 1983.

18. Rosen, M. K.; Schreiber, S. L. *Angew. Chem. Int. Ed. Engl.* **1992**, *31*, 384.

19. Michnick, S. W.; Rosen, M. K.; Wandless, T. J.; Karplus, M.; Schreiber, S. L. *Science* **1991**, *252*, 836.

20. Moore, J. M.; Peattie, D. A.; Fitzgibbon, M. J.; Thompson, J. A. *Nature (Lond.)* **1991**, *351*, 248.

21. Mierke, D. F.; Schmeider, P.; Karuso, P.; Kessler, H. *Helv. Chim. Acta* **1991**, *74*, 1027.

22. Petros, A. M.; Luly, J. R.; Liang, H.; Fesik, S. W. *J. Am. Chem. Soc.* **1993**, *115*, 9920.

23. Griffith, J. P.; Kim, J. L.; Kim, E. E.; Sintchak, M. D.; Thomson, J. A.; Fitzgibbon, M. J.; Fleming, M. A.; Caron, P. R.; Hsiao, K.; Navia, M. A. *Cell* **1995**, *82*, 507.

24. Kissinger, C. R.; Parge, H. E.; Knighton, D. R.; Lewis, C. T.; Pelletier, L. A.; Tempczyk, A.; Kalish, V. J.; Tucker, K. D.; Showalter, R. E.; Moomaw, E. W.; Gastinel, L. N.; Habuka, N.; Chen, X.; Maldonado, F.; Barker, J. E.; Bacquet, R.; Villafranca, J. E. *Nature (Lond.)* **1995**, *378*, 641.

25. Goulet, M. T.; Rupprecht, M.; Sinclair, P. J.; Wyvratt, M. J.; Parsons, W. H. *Persp. Drug Disc. Des.* **1994**, *2*, 145.

26. Liang, J.; Hung, D. T.; Schreiber, S. L.; Clardy, J. *J. Am. Chem. Soc.* **1996**, *118*, 1231.

27. Decenzo, M. T.; Park, S. T.; Jarrett, B. P.; Aldape, R. A.; Futer, O.; Murcko, M. A.; Livingston D. J. *Prot. Engng* **1996**, *9*, 173.

28. Aldape, R. A.; Futer, O.; Decenzo, M. T.; Jarrett, B. P.; Murcko, M. A.; Livingston, D. J. *J. Biol. Chem.* **1992**, *267*, 16029.

29. Yang, D.; Rosen, M. K.; Schreiber, S. L. *J. Am. Chem. Soc.* **1993**, *115*, 819.

30. Rosen, M. K.; Yang, D.; Martin, P. K.; Schreiber, S. L. *J. Am. Chem. Soc.* **1993**, *115*, 821.

31. Lepre, C. A.; Pearlman, D. A.; Cheng, J. W.; DeCenzo, M. T.; Livingston, D. J.; Moore, J. M. *Biochemistry* **1994**, *33*, 13571.

32. Mohamadi, F.; Richards, N. G. J.; Guida, W. C.; Liskamp, R.; Lipton, M.; Caufield, C.; Chang, G.; Hendrickson, T.; Still, W. C. *J. Comput. Chem.* **1990**, *11*, 440.

33. Evans, S. V. *J. Mol. Graphics* **1993**, 11, 134.

34. Pranat, J.; Jorgensen, W. L. *J. Am. Chem. Soc.* **1991**, *113*, 9483.

35. Still, W. C.; Tempczyk, A.; Hawley, R. C.; Hendrickson, T. *J. Am. Chem. Soc.* **1990**, *112*, 6127.

36. Ryckaert, E. *Mol. Phys.* **1989**, *55*, 549.

37. Wilson, K. P.; Yamashita, M. M.; Sintchak, M. D.; Rotstein, S. H.; Murcko, M. A.; Boger, J. A.; Thompson, J. A.; Fitzgibbon, M. J.; Black, J. R.; Navia, M. A. *Acta Cryst.* **1995**, *D51*, 511.

38. Connolly, P. R.; Aldape, R. A.; Bruzzese, F. J.; Chambers, S. P.; Fitzgibbon, M. J.; Itoh, S.; Livingston, D. J.; Navia, M. A.; Thomson, J. A.; Wilson K. P. *Proc. Natl. Acad. Sci. U.S.A.* **1993**, *91*, 1964

39. Itoh, S.; DeCenzo, M. T.; Livingston, D. L.; Pearlman D. A.; Navia, M. A. *Bioorg. Med. Chem. Lett.* **1995**, *5*, 1983.

(*Received in U.S.A.* 9 *July* 1996; *accepted* 15 *August* 1996)